Process optimization of Cr(VI) removal from aqueous solution using activated orange peel for treatment of tannery wastewater

Tilahun Dagnew[1,2], Zenamarkos Bantie[1,*]

[1]Chemical Engineering Program, Faculty of Chemical and Food Engineering, Bahir Dar Institute of Technology, Bahir Dar University, PO Box 26, Bahir Dar, Ethiopia
[2]Chemical Engineering Department, Engineering Faculty, University of Gondar, PO Box 196, Gondar, Ethiopia

Received: 8 April 2022 **Accepted:** 22 December 2022 **Published:** January 2023

ABSTRACT

The oxidation of trivalent chromium (Cr(III)) to more toxic hexavalent chromium (Cr(VI)) in wastewater causes several problems in aquatic environments and downstream users. The aim of this research was to optimize Cr(VI) removal from an aqueous solution using activated orange peel adsorbent for treating tannery wastewater by analyzing the effects of adsorbent dose, pH, and contact time. The design expert software was used. Raw and activated orange adsorbents were characterized by FT-IR spectroscopy, scanning electron microscope (SEM), and Brunauer-Emmett -Teller (BET). Batch adsorption experiments were carried out at room temperature and the residual concentration of Cr(VI) was analyzed by UV-VIS spectrometer. Bio-sorbent desorption was also conducted to regenerate the bio-adsorbent and recover the metal. The removal efficiency was maximum (94.74%) at pH of 2, dosage 2.5 g/L, and contact time of 90 minutes. FTIR results confirm that hydroxyl functional groups, which have high affinity towards heavy metals, are responsible for the removal of Cr(VI). Methoxy groups, which undergo demethylation to generate new hydroxyl groups after carbonization confirming oxidation, also play significant role in the adsorption process. SEM results indicate that activated orange peel adsorbent has highly porous surface created due to the removal of viscous compounds during activation. The Langmuir isotherm model shows a better fit and the reaction kinetics is described by a pseudo-second-order kinetic model ($R^2=0.99$). The Cr(VI) removal efficiency in real effluents is lower than in stock solution due to the scavenging effects of competitors. In summary, results of this research indicate that the use of activated orange peel adsorbent is promising to treat wastewater effluents for removal of Cr(VI).

Keywords: Activated Orange Peel; Chromium (VI); Adsorption; Desorption; Tannery Wastewater
DOI: https://dx.doi.org/10.4314/ejst.v16i1.4

INTRODUCTION

During the last few decades, anthropogenic activities, population growth, and poor management of natural water resources have contributed to the contamination of drinking water leading to a serious crisis reflected by the scarcity of water for

* Corresponding author: zenamarkosbs@gmail.com/Zenamarkos.Banti@bdu.edu.et

approximately half of the world's population (Jacob *et al*., 2018; Varghese *et al*., 2019). Tannery wastewater represents one of the major sources of environmental pollution since it contains many contaminants, such as heavy metals, chloride, and total organic compounds represented in biological oxygen demand (BOD) and chemical oxygen demand (COD), toxic chemicals, lime with high suspended and dissolved salts, and other pollutants (Mostafa and Peters, 2016; Saryel-Deen *et al*., 2017; Hamdy *et al*., 2019; Abdel-Aziz and Fayyadh, 2021). Heavy metal pollution from such industries, mainly chrome contamination, has a significant area of concern due to high concentrations released into the environment that can cause different health problems and is classified as carcinogenic material (Masindi and Muedi, 2018).

The sources of chromium pollution are mining, leather tanning process, cement industries, electroplating, production of steel and other metal alloys, photographic materials, corrosive paints, pigments, dyes, textiles, metal finishing, nuclear power plants, and chromate preparation (Murugesan *et al*., 2013; Tejada-Tover *et al*., 2018). Heavy metals such as chromium cause a wide range of human health effects like mutagenic and carcinogenic risks (Tejada-Tover *et al*., 2018). Large quantities of chromium (Cr) used for tanning and leather processing industries leak into aquatic environments, such as rivers and lagoons, ponds, and streams, causing water pollution and depletion of aquatic lives (Vignati *et al*., 2019). Chromium is associated with several effects on the environment and human health. Inhalation and retention of Cr(VI) containing materials can cause functional impairment to the internal organs of human beings. Skin contact with chromium (VI) leads to skin diseases (Murugesan *et al*., 2013). The operation of tanning in the leather processing industry consumes a large volume of water in several unit operations generating a massive amount of solid, gaseous, and liquid effluents that are hazardous to the environment (Mekonnen Birhanie *et al*., 2017). In chromium-tanned leather products, where Cr(III) is applied to the hides, Cr(VI) forms under certain circumstances (Chemical Information Sheet, 2021). To date, most tanneries worldwide, 80-90%, use trivalent chromium salts for tanning Bethanie (Apte *et al*., 2005; Panda *et al*., 2016). The main chromium compound used for leather tanning is chromium (III) hydroxide sulfate, $Cr(OH)SO_4$, (Apte *et al*., 2005). Chromium (III) can be oxidized to chromium (VI) at a very low pH when heated in the presence of oxygen (Apte *et al*., 2005; Swaidan *et al*., 2019). Chromium (III) in the aqueous phase can also oxidize to Cr(VI) through interaction with the manganese dioxide (MnO_2) surface (Apte *et al*., 2005). The tanning and leather processing industry results in Cr(VI) contaminated wastewater and disposal of Cr(VI) contaminated sludge (Bhavya *et al*., 2019). Wastewater from tanneries contains heavy metals and other enrichment of nutrients, especially phosphorous (P) and nitrogen (N), which reduce oxygen in the water body through intense bacterial mineralization and cause a risk to the aquatic ecosystem and makes excessive growth of algae (Nguyen *et al*., 2019). On the other hand, bio-sorption by using

peel residues from various fruits, vegetables, and plants is an ecological, versatile, simple, and economical method. If not handled properly, these residues can also contaminate the environment where they are deposited; therefore, this alternative allows the reuse of waste by incorporating multiple advantages, such as their wide availability, simple treatments, biodegradability, variety of sources, reduction of pollution, and waste management, as well as their high efficiency in the elimination of pollutants, such as heavy metals (Ranasinghe *et al*., 2018; Varghese *et al*., 2019). Orange peel stands out among these candidates due to its low cost and high content of organic compounds (pectin, cellulose, hemicellulose, among others) on its surface, along with a large amount of soluble compounds, requires a treatment that allows conditioning the biomaterial and obtaining an increase in its adsorption capacity (Chen *et al*., 2017). The orange peel that is discarded by the citrus-processing industry is characterized as having a high contaminating power, given its high content of moisture and fermentable sugars, low pH, and high content of organic matter, which gives it a high rate of fermentability, causing serious economic and environmental problems for its disposal (Patiño-Saldivar *et al*., 2021). In addition, this residue can cause soil contamination in cases of direct disposal, water pollution due to the infiltration of putrefactive residues in the water table, and air pollution due to the uncontrolled production of greenhouse gases. Consequently, the use of orange peel as a bio-sorbent material can be beneficial for the environment both by reducing waste without treatment and its effect of metal recovery.

Therefore, treating tannery wastewater using low-cost natural adsorbents is necessary to protect the aquatic environment from pollution. Furthermore, almost all researches on chrome removal have been performed on ideal conditions by preparing stock solutions from reagents of the heavy metal. This research aims to remove Cr(VI) from real tannery wastewater using activated orange peel adsorbent and optimize the adsorption process. Comparisons of chrome removal efficiencies have been investigated by considering raw orange, activated orange, and activated carbon adsorbents using both stock solutions and real tannery wastewater effluents. The preferential use of orange peel bio-sorbents is due to desired characteristics of the bio-sorbent (Kotrba *et al*., 2011) such as bio-sorption capacity due to the presence of important functional groups (such as hydroxyl and methoxy groups) which have high attraction for metal ions, economic feasibility (low cost), easy availability, easy desorption of the adsorbed metal ions, and reuse of the bio-sorbent for several cycles. Orange peel is expected to have active sites that can chelate with metal ions due to a physico-chemical process and remove these metal precipitates from aqueous solutions by filtration (Ekpete *et al*., 2010). Orange peel adsorbents were activated chemically using hydrochloric acid, which resulted in a high specific surface area that is essential for chrome removal. There are some advantages of

using hydrochloric acid over other acids like H_2SO_4, HNO_3, H_3PO_4. In aqueous environments, these acids release sulphur, nitrogen and phosphorus, respectively, causing water pollution and eutrophication. The feasibility of advanced or tertiary water treatment is also in question due to the need to remove sulphur, nitrogen and phosphorus, making the process costly. In contrast, the use of HCl provides advantages such as disinfection of aqueous solution by chlorine ion and no side effects on the aquatic environments. The effects of process variables of pH, adsorbent dosage, and contact time on the chrome removal efficiency were investigated on stock solution and optimum conditions were used to treat real tannery wastewater effluents. Adsorption isotherms and kinetics were investigated for Cr(VI) removal from wastewater. When combined with appropriate regeneration steps, adsorption is an effective method for removing toxic hexavalent chromium to reduce processing cost. Hence, desorption experiments are performed to regenerate the adsorbent, recover the metal, and to solve the problems of sludge disposal. Design expert version 7 software was used to determine the number of experimental runs and evaluate the optimum conditions for the adsorption process.

MATERIALS AND METHODS

Chemicals and equipment

All reagents used were of analytical grade. Potassium dichromate ($K_2Cr_2O_7$) was purchased from the local market to prepare the working solutions. Hydrochloric acid (HCl) was used for orange peel powder treatment. The Fourier transform infrared sample studies were performed with a Jasco FT/IR-6600, measuring from 400–4000 cm^{-1}. The textural properties of orange peel were determined using a BET parser (NOVA4000e) to measure the surface area of the adsorbent. A scanning electron microscope (FEI INSPECT F50) was used to analyze the surface morphology of raw and activated orange peel. UV-VIS spectrometry (Perkin Elmer Lambda35) was used to measure the final concentration of the metal ion remaining in the solution during the test of each batch.

Methods

Preparation of orange peel adsorbent

Orange peel samples were collected from a local market in Bahir Dar city, Ethiopia. The peels were washed with tap water to remove dirt and unwanted particles and then dried in a hot air oven at 105 ^oC for 24 h. After drying, the material was ground by laboratory mortar and pistil with particle sizes ranging from 0.150 to 0.325 mm (Pathak *et al*., 2017). The orange peel powder was carbonized with a muffle furnace at 300 ^oC for 2 h to improve porosity and adsorption efficiency.

High activation temperature above 300 ^{o}C decreases adsorption efficiency by increasing the ash content of the adsorbent and decreasing the fixed carbon content of the adsorbent (Ashtaputrey and Ashtaputrey, 2016). After carbonization and cooling, the adsorbent was soaked in hydrochloric acid (1M HCl) for 24 h at room temperature, washed with distilled water until a pH of 6-7 range was achieved, then oven dried at 105 ^{o}C up to constant mass, put in airtight bottles and stored in a desiccator for use in batch adsorption experiments (Hossain *et al*., 2012; Murugesan *et al*., 2013; Shadreck *et al*., 2013; Ayodeji *et al*., 2022).

Point of zero charge

To determine the point of zero charge of the adsorbent, 40 ml of 0.1 M KNO_3 solution was prepared in conical flasks; the pH of the solution was adjusted by using 0.1 M HCl and NaOH with the pH range of 2-10. One gram of adsorbent was added to each conical flask and shaken for 24 h using an orbital shaker. Finally, pH values were recorded after the attainment of equilibrium and pHpzc was computed based on pH changes (Pathak *et al*., 2017). The difference between initial and equilibrium pH was plotted against the initial pH of the solution. The point at which the graph crossed the x-axis was taken as pH_{pzc} value.

Characterization of adsorbent

FT-IR spectroscopy was used to identify the functional groups in the orange peel adsorbent. FT-IR spectra of the raw and activated adsorbent were recorded in the range 4000-400 cm^{-1} using a Jasco FT/IR-6600 model FT-IR spectrometer with KBr pellets.

Preparation of chromium stock solution

Standard chromium stock solution (1000 mg/L) was prepared by dissolving 2.825 g potassium dichromate ($K_2Cr_2O_7$) in 1 liter deionized water. Standard solutions for calibration and working solutions of initial metal chromium were prepared from sequential dilutions of the stock solution. For bio-sorption batch adsorption experiments, Cr solutions (100 mg/L) were prepared from the stock solution by dilution (Ekpete *et al*., 2011; Jisha *et al*., 2017).

Batch adsorption experiment

In this research, adsorbent doses of 1.5 g/L, 2 g/L, and 2.5 g/L, contact time of 30, 60, and 90 min, and pH of 2, 5, and 8 were considered for adsorption study with known initial Cr(VI) concentrations to obtain the equilibrium data. In batch tests,

the dilute Cr(VI) solution was added in 250 ml conical flasks and agitated at 120 rpm (Ekpete *et al*., 2011; Jisha *et al*., 2017; Temesgen *et al*., 2018). The required amount of adsorbent was measured by digital balance and mixed with the adsorbate solution in the conical flask. The mixture was placed on the shaker for mixing the solution. After equilibrium, the samples were filtered through Whatman No.41 filter paper and stored in the sample holder for chromium removal analysis. The filtrates were analyzed by UV-VIS spectrometry to determine the Cr(VI) concentration that remained in the solution. The amount of metal ions adsorbed by the adsorbent and the adsorption efficiency were calculated according to equations (1) to (3) (Murugesan *et al*., 2013):

$$Qe = \frac{(Co - Ce)V}{m} \quad \ldots\ldots\ldots\ldots\ldots\ldots\ldots\ldots\ldots\ldots\ldots\ldots\ldots\ldots\ldots\ldots\ldots\ldots\ldots\ldots\ldots\ldots (1)$$

$$R = \frac{(Co-Ce)}{Co} * 100 \quad \ldots\ldots\ldots\ldots\ldots\ldots\ldots\ldots\ldots\ldots\ldots\ldots\ldots\ldots\ldots\ldots\ldots\ldots\ldots\ldots\ldots\ldots (2)$$

$$Qt = \frac{Co - Ct}{m} * V \quad \ldots\ldots\ldots\ldots\ldots\ldots\ldots\ldots\ldots\ldots\ldots\ldots\ldots\ldots\ldots\ldots\ldots\ldots\ldots\ldots\ldots\ldots (3)$$

where Qe is the amount of Cr(VI) bio-sorbed per gram of biomass (mg/g); Co and Ce are the initial and equilibrium concentrations of Cr(VI) (mg/L), respectively; R is removal efficiency (%); V is constant volume of the solution (L); M is the mass of adsorbent (g); Qt is the amount of metal ion adsorbed at time t; Ct is the metal ion concentration (mg/L) at time t. The same adsorption procedure was applied for the real tannery wastewater treatment at the optimum process variables obtained from the stock solution experiments.

Langmuir adsorption isotherm model

The Langmuir isotherm assumes monolayer adsorption on a uniform surface with a finite number of adsorption sites. Once a site is filled, no further sorption can take place at that site (Maremeni *et al*., 2018). The Langmuir adsorption isotherm model was designed to quantify and contrast the adsorptive capacity of various bio-adsorbents according to (Elmorsi, 2011). The Langmuir equation can be written in the linear form as indicated in equation (4) below (Dąbrowski, 2001):-

$$\frac{C_e}{q_e} = \frac{1}{q_m K_L} + \frac{C_e}{q_m} \quad \ldots\ldots\ldots\ldots\ldots\ldots\ldots\ldots\ldots\ldots\ldots\ldots\ldots\ldots\ldots\ldots\ldots\ldots (4)$$

where C_e (mg/ L) is the equilibrium concentration of adsorbate, q_e (mg/ g) is the amount of adsorbate per unit mass of adsorbent, q_m (mg/ g) is the maximum adsorption capacity of the adsorbent and K_L (L/ mg) is Langmuir constant related to energy of adsorption.

Freundlich adsorption isotherm model

According to Freundlich's assumption, multilayer adsorption is applied and adsorbate molecules are adsorbed onto the heterogeneous surface of an adsorbent and adsorption of solutes from an aqueous phase to a solid surface is described and correlated to the amounts adsorbed per unit mass of adsorbent (Maremeni *et al*., 2018). This isotherm is applicable to adsorption processes which occur on heterogeneous surfaces (Ayawei *et al*., 2015a) and gives an expression which explains the surface heterogeneity and exponential distribution of active sites and their energies (Ayawei *et al*., 2015b).The linear form of the Freundlich isotherm is presented in equation (5) below as (Boparai *et al*. 2011):

$$logq_e = logK_F + \frac{logC_e}{n} \text{……..…….(5)}$$

Where $1/n$ is adsorption intensity. In this case, the plot of log C_e vs log q_e is employed to generate the intercept value of K_F and the slope of 1/ n.

Modeling of adsorption kinetics

The rate of chromium metal ion adsorption is analyzed by first- and second-order kinetics.

Pseudo-first-order kinetic model

Equation (6) below is the pseudo first order rate equation of the adsorption kinetics (Hossain *et al*., 2012; Kumar *et al*., 2014) and equation (7) is in its linear form (Hossain *et al*., 2012):

$$\frac{dq}{dt} = k_1(q_e - q_t) \text{ … … … … … … … … … … … … … … (6)}$$

$$\ln(q_e - q_t) = lnq_e - k_1 t \text{……..……..(7)}$$

Where k_1 is the rate constant for the pseudo-first-order kinetic equation, q_e and q_t are concentrations of solute adsorbed per unit mass of adsorbent at equilibrium and at any time t, respectively.

Pseudo-second-order kinetic model

The pseudo-second-order rate equation is presented in equation (8) below as (Kumar *et al*., 2014) and equation (9) is its linear form expression:

$$\frac{dq}{dt} = k_2(q_e - q_e)^2 \text{ … … … … … … … … … … … … (8)}$$

$$\frac{t}{q_t} = \frac{1}{k_2 {q_e}^2} + \frac{t}{q_e} \text{ … … … … … … … … … … … … (9)}$$

Where k_2 (g/mg.min) is the rate constant for the pseudo-second-order kinetic equation, q_e and q_t are concentration of solute adsorbed per unit adsorbent at equilibrium and at time t, respectively. The values of k_2 and q_e were estimated from the slope and intercept of the linear plots of t/q_t versus t.

Batch desorption

Desorption experiments were conducted after optimum conditions of adsorption. Cr(VI) solution at a concentration of 100 mg/l, pH 2.03, and 2.49 g/L of the adsorbent dose was agitated for 90 minutes using an orbital shaker at room temperature. After 90 minutes, the solution was filtered using Whatman filter paper, and the residual and adsorbed concentrations of Cr(VI) were determined. A loaded adsorbent with Cr(VI) ions was oven-dried before desorption. Then, the dried adsorbent with Cr(VI) was added to 100 ml NaOH solution (0.5 M) and agitated at 120 rpm for 90 minutes (Hossain *et al*., 2012; Mandina *et al*., 2013). This procedure was triplicated and, after each adsorption-desorption cycle, Cr(VI) recovery was evaluated by the equation (10) (Gorzin and Abadi 2018):

$$\text{Metal recovery (R)} = \frac{\text{Amount of metal ion desorbed}}{\text{Amount of metal ion adsorbed}} * 100 \quad \ldots\ldots\ldots\ldots\ldots\ldots\ldots\ldots \quad (10)$$

RESULTS AND DISCUSSION

Characterization of the biosorbent

Proximate analysis

The proximate composition of orange peel was determined to analyze its physicochemical characteristics (Table 1). The moisture content of the adsorbent affects the weight of the activated bio-sorbent, and lowering the moisture content improves adsorption efficiency because water vapor competes in the adsorption process and fills the adsorption sites within the pores reducing the adsorption efficiency of metal uptake (Zhou *et al*., 2001).

High moisture and ash contents block the active sites of the adsorbent and inhibit surface area development (Adebayo *et al*., 2016; Pakade *et al*., 2016). High ash content is undesirable for activated carbon since it reduces the mechanical strength of carbon and affects its adsorptive capacity (Ashtaputrey and Ashtaputrey, 2016). Ash content does not contribute to the development of porosity; it creates inactive sites (Martinez-Mendoza *et al*., 2020).

The volatile matter was 35.45± 0.44%, which is in close agreement with the previous study of 34.48% (Temesgen *et al*., 2018) and lower than Yadav *et al*. (2021). Volatile matter and fixed carbon content are indicators of both

carbonization degree and porosity development. During the carbonization stage, the porosity of char forms through the release of volatile matter (Martinez-Mendoza *et al*., 2020). The carbon content of the orange peel powder was 54.42%, higher than the value of Yadav *et al*., (2021).

Table 1. Moisture and ash content of adsorbent.

Moisture content		**Ash content**	
Previous studies*	**Source**	**Previous studies**	**Source**
3.5%	(Temesgen *et al*., 2018)	4.0%	(Temesgen *et al*., 2018)
3.2±0.12	(M'hiri *et al*., 2015)	5.0-6.0%	(Pathak *et al*., 2017)
10.3±0.01	(Adewole *et al*., 2014)	7.1	(Ashtaputrey and Ashtaputrey, 2016)
9.5±0.05	(Zaker *et al*., 2016)	14.4±0.35	(Zaker *et al*., 2016)
4.75	(Ashtaputrey and Ashtaputrey, 2016)	3.2±0.03	(M'hiri *et al*., 2015)
7.41	(Pathak *et al*., 2017)	5.5 ±0.02	(Adewole *et al*., 2014)
This study: 4.72±0.13%		This study: 5.5±0.05%	

PH of point of zero charge (pH_{pzc})

The point of zero charge (Pzc) for the orange peel adsorbent was 4.65 (Figure 1), acidic and a little higher than the previous study, which was 4.55 (Temesgen *et al*., 2018). If the pH of the solution is below the point of zero charge (pH < pHpzc), the surface of the adsorbent will become positively charged and attract negative ions. The highly protonated orange peel adsorbent surface electrostatically attracts oxy-anions (CrO_4^{2-}, $Cr_2O_7^{2-}$, etc.) (Gorzin and Abadi, 2018). So, dichromate ion ($Cr_2O_7^{2-}$) is adsorbed better on the surface of the adsorbent (Temesgen *et al*., 2018). If the pH of the solution is above the point of zero charge (i.e., pH >pHpzc), the surface of the adsorbent will become negatively charged and adsorption of cations is favored (Temesgen *et al*., 2018).

FT-IR analysis of bio-sorbent

As shown in Figure 2, the FT-IR spectrum of raw orange peel (dried & ground, but not carbonized and activated) shows strong hydroxyl groups (O-H) bonded with weak hydrocarbon (C-H) bonded stretching groups between 3600-2800 cm^{-1} (Nnemeka *et al*., 2016). The broad peak at 3420 cm^{-1} indicates O-H stretching vibrations in cellulose, pectin, hemicellulose, and lignin components within the orange peel adsorbent. Alcohols and phenols within the adsorbent also have O-H stretch and H-bonded stretching groups, which can adsorb Cr(VI) (Murugesan *et al*., 2013).

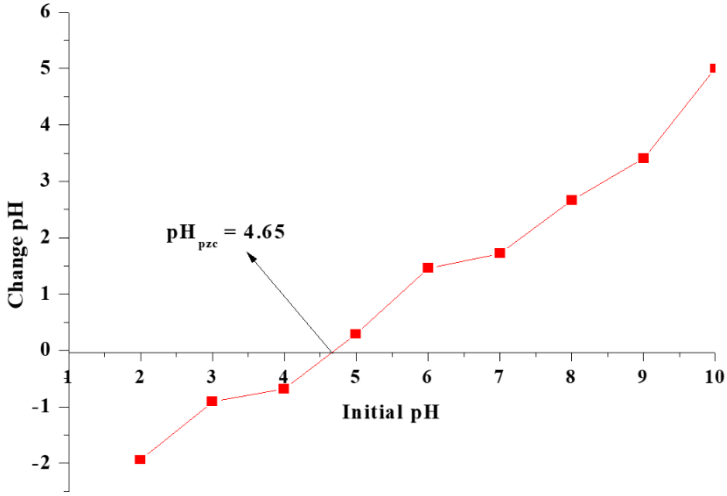

Figure 1. Point of zero charge of orange peel adsorbent

The most concentrated band in the high-energy region is due to large OH groups in the carbohydrates and the lignin of the adsorbent (Boumediene *et al*., 2015). Hydroxyl functional groups with the alcohol groups have a high affinity towards pollutants and heavy metals (Lazim *et al*., 2015). The band range between 2925 and 2927 cm^{-1} is due to C-H stretching vibration. The peak at 2918 cm^{-1} is due to C-H stretching vibrations of the methyl, methylene, and methoxy groups (Boumediene *et al*., 2015). The peak at 1744 cm^{-1} is the stretching vibration due to non-ionic carboxyl groups -COOH,-COOM, M= Na^{+}, K^{+}, Mg^{+} and Ca^{+} (Rožič *et al*., 2014). The picks within 1430-1440 cm^{-1} are due to aliphatic chains (-CH_2 and –CH_3) or possibly methoxyl groups (O-CH_3) on which lignocellulosic materials are based (Boumediene *et al*., 2015). The peaks from 1200-1400 cm^{-1} are due to symmetric stretching of -COO- of pectin (Murugesan *et al*., 2013). As shown in Figure 2, after carbonization, the HCl-treated orange peel powder shows broader picks of OH functional groups, the intensity increases due to demethylation of methoxy groups (O-CH_3) where CH_3 is replaced by the hydrogen atom and generate new OH groups (Bykov, 2008) indicating that impregnation with HCl leads to an increase in the protonation of the adsorbent surfaces.

Morphology of adsorbent

Figure 3 shows Scanning Electron Microscope (SEM) images for raw and activated orange peel powder. In these images, the morphological structures were shown for the raw and treated adsorbent via carbonization followed by activation.

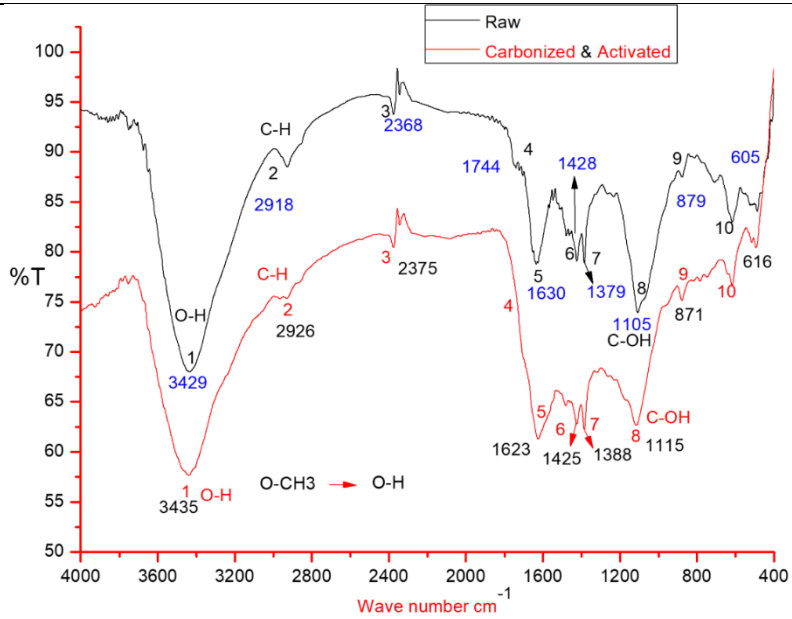

Figure 2. FT-IR spectroscopy analysis of raw and activated orange peel powder

The SEM micrographs in Figures 3a-c showed different morphologies of the raw and treated adsorbents and the presence of pores of different sizes and shapes. The raw orange peel powder (Figure 3a) shows a large and thick particle size and irregular shape with smooth walls having a small number of porosities. It is due to several viscous compounds, such as lignin and pectin, which occupy the pores of cellulose fibers (Abdel-Halim and Al-Deyab, 2012). The smooth surface indicates the presence of hydrophobic fatty and protein structures on the surface of raw orange peel powder. For activated orange peel powder (Figure 3b), the surface is highly mesoporous and irregular, which creates significant porosities for bio-sorption, with diameters in the micrometer range (Yadav *et al*., 2021). The pores are caused by evaporation of HCl during carbonization process.

Specific surface area

From the BET (NOVA4000e) analysis, for raw orange peel adsorbent, the specific surface area, pore volume, and pore diameter were obtained as 287.804 m^2/g, 0.285 cc/g, and 34.312 Å, respectively. Similarly, for activated orange peel adsorbent, these values were 473.77 m^2/g, 0.295 cc/g, and 34.32 Å, respectively. The surface area of activated orange peel adsorbent is larger than raw orange peel adsorbent and much larger than the previous studies (Murugesan *et al*., 2013; Lazim *et al*., 2015; Temesgen *et al*., 2018). This is because carbonization followed by activation

perfectly removes unnecessary components of orange peel adsorbents and increases the carbon surface.

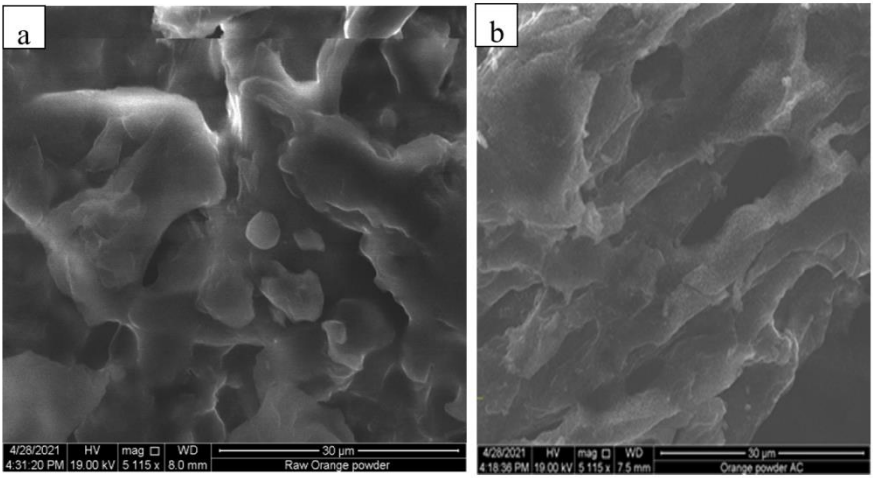

Figure 3. Morphology of orange peel: (a) raw orange peel; (b) activated orange peel.

Effect of individual process variables on Cr(VI) removal

Effect of pH

The pH of the solution is the most important process variable that significantly influences the intensity of the adsorption of Cr(VI) on a biosorbent due to the type and ionic state of the functional groups on the adsorbent surface and the chemistry of chrome in the solution (El Nemr, 2007; El Nemr, 2009). The experimental results (Figure 4a) showed that the maximum percentage removal of Cr(VI) by the orange peel adsorbent was at pH 2, which is below the point of zero charge. The favorable percentage removal of chromium (VI) ions on the adsorbent surface around this pH is due to the large concentration of H^+ ions neutralizing negatively charged hydroxyl groups (OH^-) on the adsorbent surface, thereby reducing the hindrance to the diffusion of dichromate ions (Jisha *et al*., 2017). The protonation intensity on the adsorbent surface decreases as solution pH increases resulting in a decrease in adsorption of Cr(VI) ions. At pH higher than the point of zero charge (pHpzc), the percentage removal of Cr(VI) decreases with an increase of pH due to the negative charges of the adsorbent surface causing a repulsive force with oxy-anions of chromium (Selvaraj *et al*., 2003). At higher pH values, the reduction in adsorption is due to the abundance of OH^- ions and dual competition of both anions (CrO_4^{2-} and OH^-) to the surface of the adsorbent, of which OH^- predominates (Attia *et al*., 2010; Jisha *et al*., 2017). Therefore, above the point of zero charge of the adsorbent, the percentage removal begins to fall rapidly with an increase in *pH.* Some

experimental trials were performed at pH values below 2 as the maximum adsorption was at the minimum pH selected for the experiments. From these experiments, at very acidic conditions below pH 2, adsorption efficiency was minimum (the inset figure in Figure 4a) because, at this region, dominant chromium ion ($HCrO_4^-$) and high concentration of H^+ react to form chromic acid (H_2CrO_4) which reduces the adsorption of chrome (VI) on the adsorbent surface (Tejada-Tover *et al*., 2018). As the pH of the solution reaches 2, the removal efficiency was maximum due to the highly protonated adsorbent surface enabling strong electrostatic force of attraction between the predominant species of oxy-ions (CrO_4^{2-}, $Cr_2O_7^{2-}$, etc.) and positively charged adsorbent surface (Gorzin and Abadi, 2018). In this study, the experimental data showed that the pH value of 2 gives maximum removal efficiency of Cr(VI), and it is taken as an optimum value for the other Cr(VI) adsorption experiments.

Effect of adsorbent dosage

Adsorbent dosage was selected as another main adsorption factor that determines the removal efficiency, adsorption capacity, and feasibility of the treatment process. Experimental results in Figure 4b illustrate that the percentage of Cr(VI) removal was increased from 76.16 to 94.74% when the adsorbent dosage increased from 1.5 to 2.5 g/L and maximum adsorption efficiency was recorded at a dosage of 2.5 g/L. This is because, at higher dosages of adsorbent, the active sites and surface area of adsorbent available for Cr(VI) ions adsorption increased (Jisha *et al*., 2017). In contrast, when adsorbent dosage increased beyond the optimum value, the Cr(VI) removal efficiency and adsorption capacity were decreased due to more active sites of the adsorbent that remained unsaturated during the Cr(VI) adsorption process (Radnia *et al*., 2012). In Figure 4b, a significant increase in removal efficiency was observed as dosage increases from 1.5 g/L to 2 g/L. However, when increasing dosage further, a significant increment in adsorption efficiency is not observed and the slope of the adsorption curve remains almost constant. Some adsorption experiments were performed at an adsorbent dosage higher than 2.5 g/L for confirmation, and the results showed that removal efficiency decreased due to effective surface area reduction and adsorbent aggregation (inset figure in Figure 4b) (Tejada-Tover *et al*., 2018). It has also been reported that the decrease in removal efficiency when dosage increases were due to overlapping or aggregation of the adsorbent surface area available to Cr(VI) ions and an increase in diffusion path length of adsorbate (Gönen and Serin, 2012).

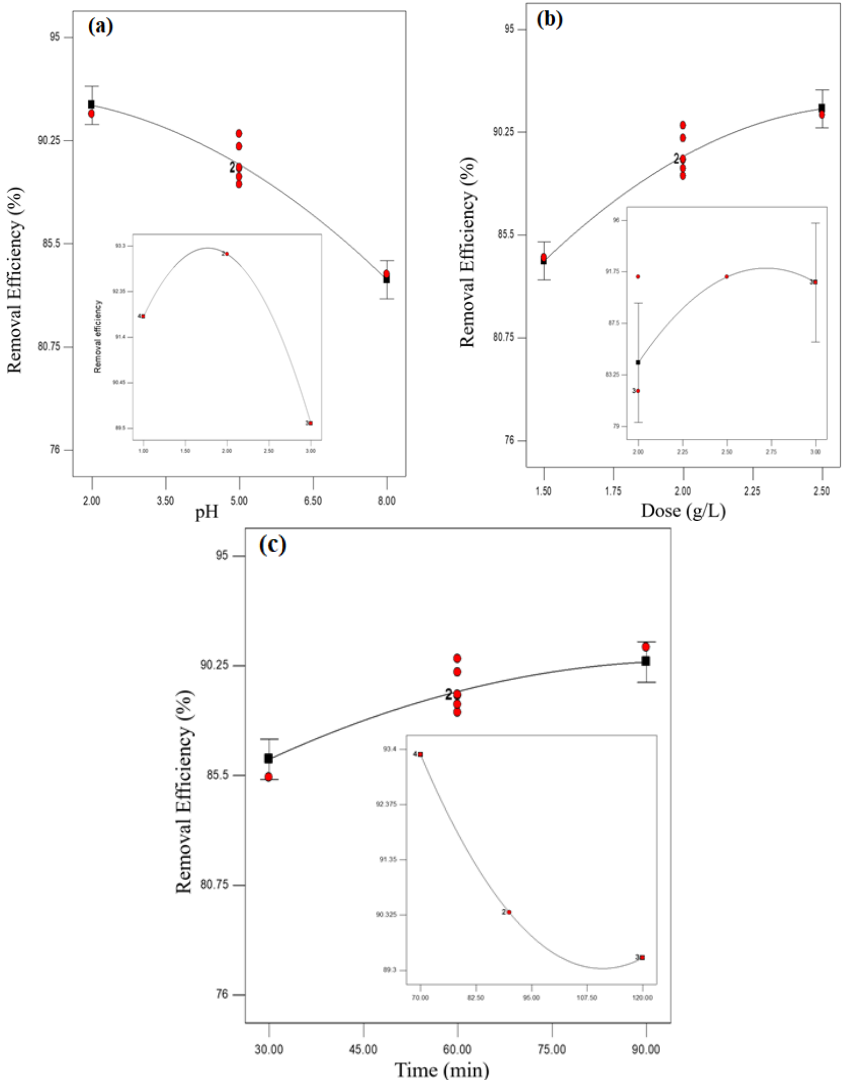

Figure 4. Effect of process variables on Cr(VI) removal efficiency by orange peel adsorbent. (a) Effect of pH. The inset figure indicates the adsorption experiment results for pH values lower than 2; (b) Effect of adsorbent dosage. The inset figure presents adsorption results for dosage higher than 2.5g/L; (c) Effect of contact time. The inset figure is the trial adsorption results at longer adsorption time, beyond the experimental range selected.

Effect of contact time

In this study, the effect of contact time on Cr(VI) removal efficiency was investigated. Figure 4c illustrates that chrome (VI) removal efficiency increases with adsorption time. It is due to the unsaturation of adsorption sites and the availability of more adsorption surface area of adsorbent (Badessa *et al*., 2020). Therefore, the concentration gradient enables the diffusion of Cr(VI) ions into the pores of the adsorbent (Kumar *et al*., 2008). In this study, as time increases, adsorption efficiency also increases smoothly, and this also suggests that sufficient contact time between adsorbent and adsorbate enables better adsorption efficiency. However, a very long contact time between adsorbent and adsorbate, above 69 minutes in this case, slows down the adsorption process as the active binding sites are filled by the Cr(VI) ions reducing removal efficiency (Badessa *et al*., 2020). Figure 4c shows a progressive adsorption process after 60 minutes, and rate of chrome removal slows down; this is due to the commencement of saturation of active sites (inset figure in Figure 4c).

Process optimization of Chromium (VI) removal

In this section, the interaction effects of process variables on Chromium (VI) removal by activated orange peel adsorbent were analyzed through three dimensional plots as shown in Figure 5, where the interaction effects of pH-dosage, pH-time, and dosage-time have been presented. The primary purpose of optimization is to determine the optimum values of parameters to maximize the response variable (chrome removal). The 3D plots show the combined effects between two reaction parameters, keeping the third variable constant at its center. From figure 5, it can be noted that the removal efficiency of Cr(VI) is sensitive to the interaction effects of all process variables. All process variables along with their interaction were significant under the specified conditions indicating that all the interaction effects are significant. The interaction effects of pH-dosage (Figure 5a) and pH-time (Figure 5b) show that the removal efficiency decreases after the intersection point; this is due to the decrease of removal efficiency as the pH increases from 2 to 8. At minimum value of pH, the removal efficiency increased when increasing of dosage from 1.5 to 2.5 g/L. On the other hand, the removal efficiency is minimum when the pH value was increased from 2 to 8 at the minimum dosage level. Figure 5b illustrates that contact time favors Cr(VI) removal efficiency more significantly than the pH of the solution. When the pH was decreased from 8 to 2, the corresponding removal efficiency was increased from 81.88 to 90.12%.

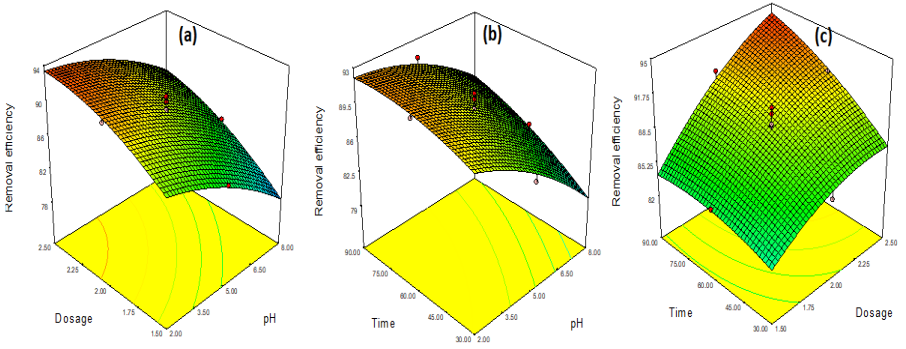

Figure 5. 3D surface plots of: (a) pH and Dosage interaction; (b) pH and contact time; (c) Dosage and Time interaction

The interaction effects of dosage and time indicate synergetic effect on removal efficiency (Figure 5c). The removal efficiency rapidly increased after their intersection point and maximum efficiency (94.74%) was achieved at their optimum levels (pH of 2, contact time of 90 min, and dosage of 2.49 g/L). Further increase of the values of the factors will have adverse effects on adsorption efficiency. For example, when the dosage is increased above optimum level, the active sites available on the surface of adsorbent remain unsaturated and no further diffusion of adsorbate onto the adsorbent will take place. This reduces the effective surface area that could be used for adsorption of the pollutant. Furthermore, aggregation of adsorbents may occur and the diffusion path length of chrome ions to the surface of the adsorbent increases at higher concentrations of adsorbent particles. Similarly, longer exposure of adsorbent to the adsorbate decreases the adsorption efficiency due to saturation of active sites of adsorbent, and desorption begins because of weakly bonded adsorbate on the adsorbent surfaces. Hence, optimum solution pH (i.e., 2), optimum adsorbent dosage (i.e., 2.5 g/L), and optimum contact time (i.e., 90 minutes) provide feasible and economical adsorption process of chromium (VI) from contaminated aqueous solution.

Patiño-Saldivar *et al*. (2021) analyzed the effect of pH on Chrome removal using orange peel adsorbent treated with water and reported that the maximum adsorption capacity is 53.15 mg/g at pH 2.72. Shadreck *et al*. (2013) investigated the effects of pH, contact time, adsorbent dose, and initial metal ion concentration for removal of Cr(VI) using orange peel treated with sodium hydroxide and found maximum adsorption capacities of 97.07 and 139.0 mg/g for raw and modified orange peels, respectively, at pH 2.0, adsorbent dosage of 4.0 mg/L, and contact time of 180 minutes. Similarly, Jisha *et al*. (2017) analyzed the effects of same factors and found that maximum Cr(VI) removal was achieved at an agitation time of 150 min, pH of 2, and initial concentration of 10 mg/l.

Adsorption isotherm

The model parameters in Table 2 show that Langmuir isotherm (Figure 6a) fitted the experimental data better than the Freundlich (Figure 6b), which illustrates orange peel adsorbent has a homogeneous surface and identical active sites (Volesky, 2001). The separation factor (SF), 0< SF<1, and adsorption capacity show favorable adsorption process fitting better with the Langmuir adsorption model (Ayawei *et al*., 2015a). Therefore, the adsorption process involves homogeneous distribution of Cr(VI) ions on active sites of the adsorbent surface through the pores of the adsorbent and the process fits well with the Langmuir adsorption isotherm (Volesky, 2001).

Table 2. Langmuir and Freundlich isotherm constant for Cr(VI) adsorption.

Langmuir model	Constant	Symbol	Value	Standard error
	Intercept	**b**	**0.3469**	**0.3616**
	Adsorption capacity	**Qm**	**5.0800**	**0.0271**
	Correlation coefficient	R^2	0.7300	-
	Energy of adsorption	Kl	0.5670	-
	Separation factor	SF	0.0800	-
	Intercept	Log kf	0.5625	0.1080
Freundlich model		Kf	3.6520	0.1080
	Adsorption intensity	N	6.0800	0.0997
	Correlation coefficient	R^2	0.0800	-

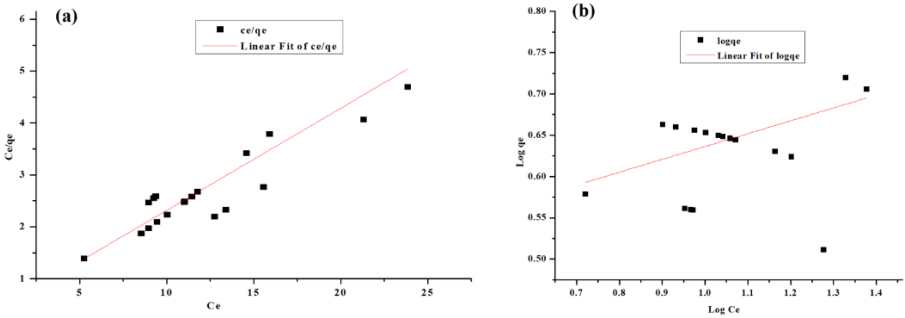

Figure 6. (a) Langmuir isotherm plot; (b) Freundlich isotherm plot

Adsorption kinetics

The study of adsorption kinetics provides an understanding of the adsorption rate. In order to determine the adsorption kinetics of Cr(VI) ion by orange peel adsorbent, pseudo-first-order (Figure 7a) and pseudo-second-order (Figure 7b) kinetic models were analyzed to fit the experimental data generated from the adsorption process. Therefore, in order to select the kinetic model which fits better, the two models were compared in terms of their R^2 and adsorption capacity values. Pseudo-second-order kinetic model (R^2 = *0.99*) shows a better correlation of experimental data, and this kinetic model is appropriate for modeling Cr(VI) adsorption onto orange peel adsorbent (Figure 7b). Pseudo-second-order kinetic model implies a chemisorption mechanism (Jisha *et al*., 2017). In this metal ion adsorption process, chemisorption is a more favorable process compared to physio-sorption, and the adsorption process is controlled by the chemisorption mechanism (Jisha *et al*., 2017).

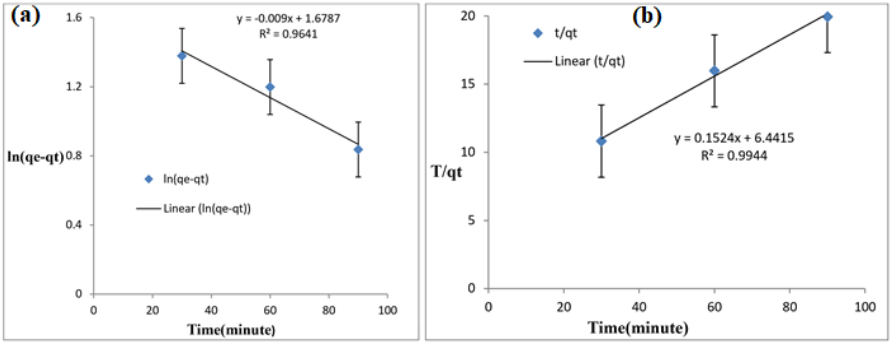

Figure 7. (a)Pseudo- first - order kinetics model; (b) Pseudo- second- order kinetics model.

Desorption and regeneration of biosorbents

After conducting an adsorption experiment, the orange peel adsorbent was desorbed off from Cr(VI) using a 0.5M NaOH desorbing agent. Desorption results showed that the maximum Cr(VI) ions were removed from the surface of the adsorbent, and the adsorbent was regenerated for another adsorption process. When successively using the regenerated adsorbent for adsorption, there was a minor variation in adsorption efficiency with the original adsorbent. This variation may be due to the mass loss of the adsorbent when used repeatedly, the minute Cr(VI) ion remaining on the active site of the adsorbent, or due to some structural damage of the adsorbent.

In Table 3, two activated orange adsorbent samples, each 2.49 g which was the optimum value by design expert software, were used to run the adsorption-

desorption experiment. The second column in Table 3 was the absorbance of activated adsorbent for samples 1 & 2 with triplication. Column three indicates the remaining chromium concentration in the filtrate, and column four the amount of chromium loaded on the surface of the adsorbent, which is an initial concentration for the desorption study. After desorption using 0.5 M NaOH, it gives high desorption absorbance (column 6), implying that a high concentration of chromium is desorbed from the loaded adsorbent (column7), and the adsorbent was regenerated (chromium-free). When using the regenerated adsorbent, the absorbance increased for samples 1 (from 0.22 to 0.296) and 2 (from 0.194 to 0.225). It could be related to the mass loss of the adsorbent and some remaining Cr(VI) on the active site of the adsorbent.

Table 3. Batch adsorption and desorption result

No of run	Adsorption			Desorption			*R** (%)
	Absorbance	Remain Ce(ppm)	Adsorbed Ce (ppm)	Initial Co(ppm)	Absorbance	Desorbed Ce(ppm)	
1	0.220	7.33	92.67	92.67	2.55	85.13	91.87
	0.258	8.60	91.40	91.47	2.47	82.20	89.93
	0.296	9.87	90.13	90.13	2.59	86.37	95.82
2	0.194	6.47	93.53	93.50	2.63	87.67	93.73
	0.224	7.46	92.54	92.54	2.70	90.03	97.29
	0.225	7.50	92.50	92.50	2.75	91.77	99.21

*R(%) is the percentage metal recovery.

Table 3 shows that maximum metal recovery was achieved from the desorption confirming the weakly bonded interaction between activated orange peel adsorbent and hexavalent chromium (adsorbate), the adsorption process is reversible with pseudo-second-order, and monolayer adsorption is easier to desorb the adsorbent. Re-using these bio-sorbents several times without damaging the active surface makes the treatment process feasible and protects the environment from pollution.

Treatment of real tannery wastewater effluent

In this research work, we addressed the adsorption efficiency of activated orange peel on actual tannery wastewater effluent. Almost all the experimental research works related to removal of heavy metals from wastewater are conducted by preparing stock solution using the metallic reagent. More specifically, experiments on removal of chromium (VI) are performed by preparing stock solution from potassium dichromate reagent. In this work, after investigating the adsorption potential of orange peel (*Citrus cinensis*) adsorbent using stock solution, experiments were also conducted on real tannery wastewater effluents from Bahir

Dar tannery and leather processing industry. The experiments on real tannery effluent were conducted at the optimum values of process variables (adsorbent dosage of 2.5 g/L, pH of 2, and contact time of 90 min) obtained from stock solution adsorption. Table 4 below indicates raw orange, activated orange, and commercial activated carbon adsorbents removal efficiencies on artificial wastewater (stock solution) and actual tannery wastewater effluents. It can be noted that the adsorption efficiency of activated orange is significantly higher than raw orange adsorbent (i.e., Raw orange < Activated orange < commercial activated carbon) on both stock and real tannery effluents. Furthermore, chromium (VI) was adsorbed better on stock solution than real effluents because of the presence of other competitors with chromium in the effluent and due to their scavenging effects in real tannery wastewater. Further study is needed on the improving of the adsorption efficiency of biosorbents for reamoval of heavy metals from real tannery wastewater and develop feasible treatment technology.

Table 4. Comparison of Cr(VI) removal efficiencies of raw orange, activated orange, and activated carbon adsorbents

Adsorbent type	Solution (ml)	Dose (g)	pH	Time (min)	Initial Cr(VI) (ppm)	Final (ppm)	Efficiency (%)
Raw orange	Stock	2.49	2.03	90.00	100.00	26.78	73.20
	Raw tannery effluent	2.49	2.03	90.00	46.71	32.27	30.92
Activated orange	Stock	2.49	2.03	90.00	100.00	5.26	94.74
	Raw tannery effluent	2.49	2.03	90.00	46.71	13.10	72.41
Activated carbon	Raw tannery effluent	2.49	2.03	90.00	46.71	5.34	88.56

CONCLUSION

In this study, the chemical modification of orange peel with HCl resulted in significant increase in the removal efficiency of Cr(VI). FT-IR and SEM analysis of activated orange peel adsorbent showed different functional groups and surface morphology, respectively. The efficiency of the adsorption process was strongly dependent on the pH, adsorbent dosage, and contact time. The maximum removal efficiency of Cr(VI) was 94.74% at pH of 2, adsorbent dosage of 2.5 g/L, and contact time of 90 minutes. The adsorption isotherm equilibrium data were fitted by Langmuir and Freundlich isotherms, and the Langmuir model shows better correlation; this indicates that the orange peel adsorbent has homogeneous and

identical active sites and the adsorption process is a monolayer. Adsorption kinetics equilibrium data were analyzed using pseudo-first-order kinetics and pseudo-second-order kinetic models, and the latter shows a better fit; this indicates the adsorption of Cr(VI) on orange peel adsorbent is a chemisorption mechanism. Furthermore, regeneration of orange peel adsorbent was conducted, and the adsorption potential of regenerated adsorbent shows a minor variation with the original adsorbent. It confirms that the adsorption process is reversible with pseudo-second-order kinetics and monolayer adsorption, implying that the interaction between activated orange peel adsorbent and Cr(VI) is weak. The bio-sorbents can be used several times making the treatment process feasible and protecting the environment from pollution. The adsorption experiments on real tannery wastes gave promising results and further research works are needed to improve the chrome removal efficiency.

ACKNOWLEDGEMENTS

The authors thank the Faculty of Chemical and Food Engineering, Bahir Dar Institute of Technology, Bahir Dar University, Ethiopia allowing us to use the laboratory materials, chemicals, and instruments.

DECLARATIONS

Authors' contributions

All the authors contributed to all experimental activities, manuscript writing, editing, reviewing and approved the final manuscript.

Conflict of interest

All authors have read and understood the policy of the competing interests and declare that there are no competing interests.

Funding

This work has been funded by Bahir Dar Institute of Technology, Bahir Dar University, Ethiopia (www.bdu.edu.it).

Ethical statement

This work did not involve humans and animals and no ethical declarations were needed.

REFERENCES

Abdel-Aziz, H.M and Fayyadh, S.N. (2021). Removal of orange G by the Fenton process and *Ficus benjamina* nano-zerovalent iron. *Journal of Environmental Engineering and Science* **40**: 1–8. https://doi.org/10.1680/jenes.20.00044

Abdelhalim, E.S and Al-deyab, S.S. (2012). Chemically modified cellulosic adsorbent for divalent cations removal from aqueous solutions. *Carbohydrate Polymers* **87**(2): 1863-1868. https://doi.org/10.1016/j.carbpol.2011.10.028

Adebayo, G.B., Mohammed, A.A and Sokoya, S.O. (2016). Biosorption of Fe (II) and Cd (II) ions from aqueous solution using a low cost adsorbent from orange peels. *Journal of Applied Sciences and Environmental Management* **20**(3): 702-714. http://dx.doi.org/10.4314/jasem.v20i3.25

Adewole, E., Adewumi, D.F., Jonathan, J and Fadaka, A. (2014). Phytochemical constituents and proximate analysis of orange peel (citrus fruit). *Journal of Advanced Botany and Zoology* **1**(3): 3–5. https://doi.org/10.5281/zenodo.999929.

Apte, A.D., Verma, S., Tare, V and Bose, P. (2005). Oxidation of Cr (III) in tannery sludge to Cr(VI) field observations and theoretical assessment. *Journal of Hazardous Materials* **121**: 215–222. https://doi.org/10.1016/j.jhazmat.2005.02.010.

Ashtaputrey, S.D. and Ashtaputrey, P.D. (2016). Preparation and characterization of activated charcoal derived from orange peel. *Journal of Advanced Chemical Sciences* **2**(3): 360–362.

Attia, A.A., Khedr, S.A., Elkholy, S.A. (2010). Adsorption of chromium ion (VI) by acid activated carbon. *Brazilian. Journal of Chemical Engineering* **27**(1): 183–193. https://doi.org/10.1590/S0104-66322010000100016.

Ayawei, N., Angaye, S.S., Wankasi, D., Dikio, E.D. (2015a). Synthesis, characterization and application of mg/Al layered double hydroxide for the degradation of congo red in aqueous solution. *Open Journal of Physical Chemistry* **5:** 56-70. http://dx.doi.org/10.4236/ojpc.2015.53007.

Ayawei, N., Ekubo, A. T., Wankasi, D., & Dikio, E. D. (2015b). Adsorption of congo red by Ni/Al-CO3: equilibrium, thermodynamic and kinetic studies. *Oriental Journal of Chemistry* **31**(3): 1307–1318. https://doi.org/10.13005/ojc/310307

Ayodeji, A., Bamidele, D., Sunday, F., Oluranti, A and Edith, A. (2022). Corrosion inhibitive performance of the waste orange peels (*Citrus sinensis*) on A36 mild steel in 1M HCl. 17. https://doi.org/10.20964/2022.01.36

Badessa, T.S., Wakuma, E and Yimer, A.M. (2020). Bio-sorption for effective removal of chromium(VI) from wastewater using Moringa stenopetala seed powder (MSSP) and banana peel powder (BPP). *BMC Chemistry* **14**(1): 1–12. https://doi.org/10.1186/s13065-020-00724-z.

Bhavya, K.S., Raji, P., Selvarani, J.A., Samrot, A.V., Javad, P.T.M., Appalaraju, V.S. (2019). Leather processing, its effects on environment and alternatives of chrome tanning. *International Journal of Advanced Research in Science, Engineering and Technology* **10**(6): 69–79. http://dx.doi.org/10.34218/IJARET.10.6.2019.009.

Boparai, H.K., Joseph, M and O'Carroll, D. M. (2011). Kinetics and thermodynamics of cadmium ion removal by adsorption onto nano zerovalent iron particles. *Journal of Hazardous Materials* **186**(1): 458–465. https://doi.org/10.1016/j.jhazmat.2010.11.029

Boumediene, M., Benaïssa, H., George, B., Molina, St., Merlin, A. (2015). Characterization of two cellulosic waste materials (orange and almond peels) and their use for the removal of methylene blue from aqueous solutions. *Madera Cienciay tecnología* **17**(1): 69–84. http://dx.doi.org/10.4067/S0718-221X2015005000008.

Bykov, I. (2008). Characterization of natural and technical lignins using FTIR spectroscopy. Master Thesis, Lulea University of Technology, Sweden.

Chemical Information Sheet (2021). Chromium (VI) March, pp 3–5.

Chen, H., Dou, J and Xu, H. (2017) Removal of Cr(VI) ions by sewage sludge aqueous compost biomass from solutions: Reduction to Cr(III) and biosorption. *Applied Surface Scieince* **425:** 728–735. https://doi.org/10.1016/j.apsusc.2017.07.053

Dąbrowski, A. (2001). Adsorption - From theory to practice. *Advances in Colloid and Interface Science* **93**(1–3): 135–224. https://doi.org/10.1016/S0001-8686(00)00082-8

Ekpete, O.A., Kpee, F., Amadi, J.C and Rotimi, R.B. (2010). Adsorption of chromium (VI) and zinc (II) ions on the skin of orange peels (*Citrus sinensis*). *Journal of Nepal Chemical Society* **26**: 31–39. https://doi.org/10.3126/jncs.v26i0.3628.

Elmorsi, T.M. (2011). Equilibrium isotherms and kinetic studies of removal of methylene blue dye by adsorption onto miswak leaves as a natural adsorbent. *Journal of Environmental Protection* **02**(06): 817–827. https://doi.org/10.4236/jep.2011.26093

El Nemr, A. (2007). Pomegranate husk as an adsorbent in the removal of toxic chromium from wastewater. *Chemistry and Ecology* **23**(5): 409–425. https://doi.org/10.1080/02757540701653350

El Nemr, A. (2009). Potential of pomegranate husk carbon for Cr(VI) removal from wastewater: kinetic and isotherm studies. *Journal of Hazardous Materials* 161:132–141. https://doi.org/10.1016/j.jhazmat.2008.03.093.

Gönen, F and Serin, D.S. (2012). Adsorption study on orange peel removal of Ni(II) ions from aqueous solution. *African Journal of Biotechnology* **11**(5): 1250–1258. https://doi.org/10.5897/ajb11.1753.

Gorzin, F and Abadi, M.B.R. (2018). Adsorption of Cr(VI) from aqueous solution by adsorbent prepared from paper mill sludge: Kinetics and thermodynamics studies. *Adsorption Science and Technology* **36**: 149–169. https://doi.org/10.1177/0263617416686976.

Hamdy, A., Mostafa, M and Nasr, M. (2019). Regression analysis and artificial intelligence for removal of methylene blue from aqueous solutions using nanoscale zero-valent iron. *International Journal of Environmental Science and Technology* **16**(1): 357–372. https://doi.org/10.1007/s13762-018-1677-z.

Hossain, M.A., Ngo, H.H., Guo, W.S and Nguyen, T.V. (2012). Removal of copper from water by adsorption onto banana peel as bioadsorbent. *International Journal of Geotechnique, Construction Materials and Environment* **2**(2): 227–234.

Jacob, J.J., Varalakshmi, R., Gargi, S and Jayasri, M.A. (2018). Suthindhiran, K. removal of Cr (III) and Ni (II) from tannery effluent using calcium carbonate coated bacterial magnetosomes. *Clean Water* **1**: 1–10. https://doi.org/10.1038/s41545-018-0001-2.

Jisha, T.J., Lubna, C.H and Habeeba, V. (2017). Removal of Cr(VI) using orange peel as an adsorbent. *International Journal Advance Research Innovative Ideas in Education* **3**(4): 276–283.

Kotrba, P., Mackova, M and Macek, T. (2011). Microbial biosorption of metals. Springer Books, Dordrecht.

Kumar, R., Bishnoi, N.R., Sharma, G., and Bishnoi, K. (2008). Biosorption of chromium(VI) from aqueous solution and electroplating wastewater using fungal biomass. *Chemical Engineering Journal* **135**(3): 202–208. http://dx.doi.org/10.1016/j.cej.2007.03.004.

Kumar, P.S., Fernano, P.S.A., Ahmed, R.T., Srinath, R., Priyadharshini, M., Vignesh, A.M., and Thanjiappan, A. (2014). Effect of temperature on the adsorption of methylene blue dye onto sulfuric acid–treated orange peel. *Chemical Engineering Communications* **201**(11), pp. 1526–1547. doi: 10.1080/00986445.2013.819352.

Lazim, Z.M., Mazuina, E., Hadibarata, T and Yusop, Z. (2015). The removal of methylene blue and remazol brilliant blue r dyes by using orange peel and spent tea leaves. *Journal Teknologi* **74**(11). https://doi.org/10.11113/jt.v74.4882.

Mandina, S., Chigondo, F and Shumba, M. (2013). Removal of chromium (VI) from aqueous solution using chemically modified orange (*Citrus cinensis*) peel. IOSR Journal of Applied Chemistry.6(2): 66-75.

Maremeni, L.C., Modise, S.J., Mtunzi, F.M., Klink, M.J and Pakade, V.E. (2018). Adsorptive removal of hexavalent chromium by diphenylcarbazide-grafted macadamia nutshell powder. *Bioinorganic Chemistry and Applications* 2018(i). https://doi.org/10.1155/2018/6171906

Martínez-Mendoza, K.L., Barraza-Burgos, J.M., Marriaga-Cabrales, N., Machuca-Martinez, F., Barajas, M and Romero, M. (2020). Production and characterization of activated carbon from coal for gold adsorption in cyanide solutions. *Ingenier´Ia E Investigacion* **40**(1): 34-44. http://dx.doi.org/10.15446/ing.investig.v40n1.80126.

Masindi, V., & Muedi, K. L. (2018). Environmental contamination by heavy metals. In Heavy Metals (pp. 115-133). IntechOpen. https://doi.org/10.5772/intechopen.76082

M'hiri, N., Ioannou, I., Ghoul, M., Mihoubi and Boudhrioua, N. (2015). Proximate chemical

composition of orange peel and variation of phenols and antioxidant activity during convective air drying. *Js-Inat* **9**: 881–890. Available: www.jnsciences.org.

Mekonnen Birhanie, Seyoum Leta and Khan, M.M. (2017). Treatment of tannery wastewater to remove hazardous pollutants by scoria (volcanic ash) a low-cost adsorbent. *International Journal of Environment, Agriculture and Biotechnology* **2**(6): 2841–2849. http://dx.doi.org/10.22161/ijeab/2.6.10.

Mostafa, M.K and Peters, R.W. (2016). Improve effluent water quality at Abu-Rawash wastewater treatment plant with the application of coagulants. *Water and Environment Journal* **30**(1–2): 88–95. https://doi.org/10.1111/wej.12161.

Murugesan, A., Vidhyadevi, T., Kirupha, S.D., Ravikumar, L and Sivanesan, S. (2013). Removal of chromium (VI) from aqueous solution using chemically modified corncorb-activated carbon: Equilibrium and kinetic studies. *Environmental Progress & Sustainable Energy* **32**(3): 673–680. https://doi.org/10.1002/ep.11684.

Nguyen, T.N., Némery, J., Gratiot, N., Strady, E., Tran, V.Q., Nguyen, A.T., Aimé, J and Peyne, A. (2019). Nutrient dynamics and eutrophication assessment in the tropical river system of Saigon – Dongnai (southern Vietnam). *Science of the Total Environment* **653**: 370–383. https://doi.org/10.1016/j.scitotenv.2018.10.319.

Nnemeka, I., Godwin, E., Olakunle, F., Olushola, O., Moses, O., Chidozie, O.P and Rufus, S. (2016). Microwave enhanced synthesis of silver nanoparticles using orange peel extracts from Nigeria. *Chemical and Biomolecular Engineering* **1**(1): 5–11. https://doi.org/10.11648/j.cbe.20160101.12.

Pakade, V.E., Maremeni, L.C., Ntuli, T.D and Tavengwa, N.T. (2016). Application of quaternized activated carbon derived from macadamia nutshells for the removal of hexavalent chromium from aqueous solutions. *South African Journal of Chemistry* **69**: 180–188. http://dx.doi.org/10.17159/0379-4350/2016/v69a22.

Panda, R.C., Selvasekhar, S., Murugan, D., Sivakumar, V., Narayani, T and Sreepradha, C. (2016). Cleaner production of basic chromium sulfate - With a review of sustainable green production options. *Journal of Cleaner Production* **112:** 4854–4862. https://doi.org/10.1016/j.jclepro.2015.05.123

Pathak, P.D., Mandavgane, S.A and Kulkarni, B.D. (2017). Fruit peel waste: characterization and its potential uses. *Current Science* **113**(3): 444-454. https://doi.org/10.18520/cs/v113/i03/444-454.

Patiño-Saldivar, L., Hernández, J.A., Ardila, A., Salazar-Hernández, M., Talavera, A and Hernández-Soto, R. (2021). Cr (III) removal capacity in aqueous solution in relation to the functional groups present in the orange peel (*Citrus sinensis*). *Applied Sciences* **11:** 6346. https://doi.org/10.3390/app11146346

Radnia, H., Ghoreyshi, A.A., Younesi, H and Najafpour, G.D. (2012). Adsorption of Fe(II) ions from aqueous phase by chitosan adsorbent: Equilibrium, kinetic and thermodynamic studies. *Desalination and Water Treatment* **50**(1–3): 348–359. https://doi.org/10.1080/19443994.2012.720112.

Ranasinghe, S.H., Navaratne, A.N and Priyantha, N. (2018) Enhancement of adsorption characteristics of Cr(III) and Ni(II) by surface modification of jackfruit peel biosorbent. *Journal of Environmental and Chemical Engineering* **6**: 5670–5682. https://doi.org/10.1016/j.jece.2018.08.058.

Rožič, M., Senji, I.R.A and Miljanić, S. (2014). Methylene blue sorption characterization onto orange and lemon peels. *The Holistic Approach to Environment* **4**(3): 97-110.

Saryel-Deen, R.A., Mahmoud, A.S., Mahmoud, M., Mostafa, M.K and Peters, R. W. (2017). Adsorption and kinetic studies of using entrapped sewage sludge ash in the removal of chemical oxygen demand from domestic wastewater, with artificial intelligence approach. The Annual AIChE Meeting, Minneapolis, MN, United States.

Selvaraj, K., Manonmani, S and Pattabhi, S. (2003). Removal of hexavalent chromium using distillery sludge. *Bioresource Technology* **89**(2): 207–211. https://doi.org/10.1016/S0960-8524(03)00062-2.

Shadreck, M., Chigondo, F., Shumba, M., Benias, C., Nyamunda, E and Dube, E. (2013). Removal of chromium (VI) from aqueous solution using chemically modified orange (*Citrus cinensis*) peel. *International Organization of Scientific Research, Journal of Applied Chemistry* **6**: 66-75.

Swaidan, A., Borthakur, P., Boruah, P.K., Das, M.R., Barras, A., Hamieh, S and Boukherroub, R. (2019). A facile preparation of CuS-BSA nanocomposite as enzyme mimics: application for

selective and sensitive sensing of Cr(VI) ions. *Sensors and Actuators B. Chemical* **294**: 253–262. https://doi.org/10.1016/j.snb.2019.05.052.

Tejada-Tovar, C., Gonzalez-Delgado, A.D and Villabona-Ortiz, A. (2018) Removal of Cr(VI) from aqueous solution using orange peel-based biosorbents. *Indian Journal of Science and Technology* **11**(13): 1-13. http://dx.doi.org/10.17485/ijst/2018/v11i13/121602.

Temesgen, F., Gabbiye, N and Sahu, O. (2018). Biosorption of reactive red dye (RRD) on activated surface of banana and orange peels: Economical alternative for textile effluent. S*urfaces and Interfaces* **12**: 151-159. https://doi.org/10.1016/j.surfin.2018.04.007.

Varghese, A.G., Paul, S.A., Latha, M.S. (2019). Remediation of heavy metals and dyes from wastewater using cellulose-based adsorbents. *Environmental Chemistry Letters* **17:** 867–877. https://doi.org/10.1007/s10311-018-00843-z.

Vignati, D.A.L., Ferrari, B.J.D., Roulier, J.L., Coquery, M., Szalinska, E., Bobrowski, A., Czaplicka, A., Kownacki, A and Dominik, J. (2019). Chromium bioavailability in aquatic systems impacted by tannery wastewaters. *Science of the Total Environment* **653**: 401–408. https://doi.org/10.1016/j.scitotenv.2018.10.259.

Volesky, B. (2001). Detoxification of metal-bearing effluents: biosorption for the next century. *Hydrometallurgy* **59**(2–3): 203–216. https://doi.org/10.1016/S0304-386X(00)00160-2.

Yadav, P and Gupta, V.C. (2021). Comparative study on biosorption of arsenite ions onto raw and chemically activated orange peel powder in batch reactor. *International Journal of Engineering, Science and Technology* **13**(1): 158–170. http://dx.doi.org/10.4314/ijest.v13i1.24S.

Zaker, M.A., Sawate, A.R., Patil, B.M and Sadawarte, S.K. (2016). Studies on effect of orange peel powder incorporation on physical, nutritional and sensorial quality of cookies. *International Journal of Engineering Research & Technology* **5**(9): 78–82. http://dx.doi.org/10.17577/IJERTV5IS090125.

Zhou, L., Sun, Y and Zhou, Y. (2001). Effect of moisture in microporous activated carbon on the adsorption of methane. *Carbon* **39**(5): 773-776. https://doi.org/10.1016/S0008-6223(01)00025-2.